

A hybrid approach for power quality monitoring

Okan ÖZGÖNENEL^{1,*}, Ümit Kemalettin TERZİ², Abdesh KHAN³

¹*Department of Electrical & Electronics Engineering, Faculty of Engineering,
Ondokuz Mayıs University, 55139 Kurupelit, Samsun-TURKEY
e-mail: okanoz@omu.edu.tr*

²*Department of Electrical Education, Marmara University, İstanbul-TURKEY
e-mail: ukterzi@hotmail.com*

³*Husky Injection Molding Systems Ltd., Bolton, Ontario-CANADA
e-mail: abkhan@husky.ca*

Received: 21.02.2011

Abstract

This paper presents a novel hybrid approach for detection of power quality (PQ) disturbances. The proposed hybrid algorithm is based on applications of principle component analysis, discrete wavelet transform, and fast Fourier transform on voltage and current waveforms. The proposed PQ monitoring (PQM) software uses 3-phase voltage and current signals in order to detect possible power disturbances such as voltage sag, flicker, harmonics, transients, DC component, and electromagnetic interference. The test results demonstrate the potential of the proposed hybrid technique for PQM and PQ assessment.

Key Words: *Power quality, discrete wavelet transform, principal component analysis, fast Fourier transform, instrumentation*

1. Introduction

Power quality (PQ) problems are one of the main concerns for utilities and manufacturing industries. PQ events are defined in IEEE Standard 1159 using voltage and current signals for power system monitoring [1]. PQ is not just an indicator in order to help the utilities save costs, but is also an indicator of quality and reliable services to the customers [2]. A good knowledge of PQ events can help power companies to choose proper equipment. Therefore, power and utility companies perform PQ surveys in order to gather real-time PQ information [3-5]. Computers and communication-related electronic equipment are more sensitive to power disturbances that occur both on the power system and within customer amenities. Moreover, with a huge application of power electronics equipment such as solid-state switching devices, lighting controls, industrial plant rectifiers and inverters, and distributed generation power converters, the harmonic pollution for utilities becomes more serious. Power electronic loads cause serious harmonic voltage distortions, large inrush currents with excessive harmonics, and high distortions [6].

*Corresponding author: Department of Electrical & Electronics Engineering, Faculty of Engineering, Ondokuz Mayıs University, 55139 Kurupelit, Samsun-TURKEY

PQ problems also cause equipment malfunction, data loss, programmable logical controller malfunctions, and sensitive load blackout. From an economic point of view, utilities face higher costs due to degraded PQ. For these reasons, PQ monitoring (PQM) and analysis is becoming a major challenge. PQ and reliability issues are very important to the successful delivery of electrical energy. Loss of voltage has serious economic consequences. Therefore, utilities are required to provide the highest reliability and PQ in a deregulated environment [7,8].

Recently, many PQM techniques have been proposed to detect disturbances. These techniques can be summarized as:

- Those based on a personal computer or digital signal processor with advanced commercial software like MATLAB™, LabVIEW, or general programming languages like C++ [6,9-12],
- Instance virtual instruments, which are based on general packet radio service and LabVIEW software [2,13,14],
- Web-based PQM systems using a commercial PQ meter like HIOKI 3196 [15,16], and
- Signal processing algorithms such as wavelets, fast Fourier transform (FFT), and empirical mode decomposition [7,8,17,18].

The above algorithms and identification techniques are used for detecting limited PQ disturbances (PQDs) such as voltage sag/swell, momentary interruption, and harmonics. Some algorithms are based on Kalman filtering, instantaneous voltage vector, and indirect demodulation methods, including detection of voltage flicker [19-21]. Most of these techniques are not able to give useful information such as the beginning and ending of the problem and the magnitudes and frequencies of voltage flicker/harmonics during a PQD. The proposed hybrid algorithm is able to detect PQ problems such as voltage sag/swell, momentary interruption, transients, harmonics, electromagnetic interferences, and DC component. As soon as a PQ problem is detected in the decision-making unit, the post calculation is performed in order to give information about the problem. The proposed algorithm consists of the following 2 calculation steps:

- Feature vectors are obtained from 3-phase voltage and current signals using the discrete wavelet transform (DWT) and principle component analysis (PCA). A 3-phase pure sine signal is used to represent a healthy condition, and then DWT coefficients of the disturbance signals are compared with the healthy ones. Since DWT coefficients in the frequency range of 49.5-50.5 Hz cause wrong decisions for voltage sag/swell, the PCA technique is applied in order to remove the confusion.
- Local maxima and minima are calculated to extract the envelope of each signal in the decision-making unit. The proposed PQD detection technique can be decomposed into the following 3 steps:
 - Testing the algorithm for PQDs. Generation of PQ events consists of mathematical equations and simulation studies.
 - Obtaining power system voltage/current waveforms using software from the Scientific and Technological Research Council of Turkey (TÜBİTAK) in order to test the algorithm [3,4].
 - Running the decision-making unit for the extracted feature vectors.

The paper is organized as follows: Section 2 describes discrete wavelet analysis and feature vector extractions using the DWT; Section 3 describes PCA and feature vector extractions using PCA; Section 4 explains the calculation procedure and decision-making unit; and Section 5 gives the examples of real-time studies where the sampling frequency is chosen as 25.6 kHz, in compliance with the TÜBİTAK data.

2. Discrete wavelet transform

The DWT is used to extract transients of the analyzed signal. The DWT approach has been widely used in engineering signal processing applications over the past decade. The main advantage of the DWT is that it has a varying window size, which is wide for low frequencies and narrow for high frequencies, leading to an optimal time-frequency resolution in all frequency ranges [17-22]. In this study, the DWT calculation is required to obtain distinctive attributes (local discontinuities) from voltage and current samples in the data window. The DWT of a signal x is calculated by passing it through a series of filters. First, the samples are passed through a low-pass filter with impulse response g , resulting in a convolution of the input signal and low-pass filter. It can be represented as:

$$y[n] = (x * g)[n] = \sum_{k=1}^n x[k]g[n - k]. \tag{1}$$

In Eq. (1), x is the normalized voltage signal. The signal is also decomposed simultaneously using a high-pass filter with impulse response h . The outputs are the detail coefficients (from the high-pass filter) and approximation coefficients (from the low-pass filter). It is important that the 2 filters are related to each other, and they are known as a quadrature mirror filter. However, it is not always necessary that they be a quadrature mirror filter. The filter outputs can be rewritten as:

$$y_{low_freq}[n] = \sum_{k=1}^n x[k]g[2n - k], \tag{2}$$

$$y_{high_freq}[n] = \sum_{k=1}^n x[k]h[2n + 1 - k]. \tag{3}$$

Eqs. (2) and (3) describe the basic DWT computational step followed by decimation by 2. This decimation technique is operated to optimize the architecture for a one-dimensional DWT. The decomposition has halved the time resolution, since only half of each filter output characterizes the signal. However, each output has half of the frequency band of the input. For multirate analysis, the decomposition is repeated and the approximation coefficients are further decomposed with high- and low-pass filters.

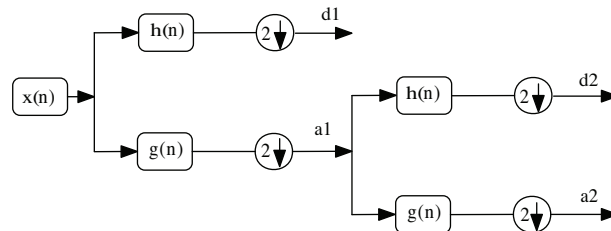


Figure 1. Classical wavelet tree based on Mallat's algorithm.

This is represented as a binary tree with nodes representing a subspace with different time-frequency localizations. The tree is known as a filter bank [23-24]. Figure 1 shows the decomposition tree.

In this study, the minimum description length (MDL) data criterion [30] is used for the selection of wavelet function. The MDL data criterion is applied to the simulation and real-time data from TÜBİTAK. The Shannon entropy-based criterion is used in this study in order to find the optimum level of resolution of the proposed PQM system. The entropy-based criterion calculates the entropy of each subspace consisting of detail coefficients (d) and approximation coefficients (a) at each level of resolution of the DWT. It compares the entropy of a parent subspace with those of its children's subspaces in order to find the optimum level of resolution using the optimum mother wavelet. The criterion states that if the entropy of a signal at a new level is higher than that at the previous level, the decomposition of the signal is not needed.

2.1. Feature extraction

To distinguish different types of disturbances in power systems, it is essential to perform additional processing of the original signals. For this purpose, the eighth-order Daubechies ($db8$) wavelet filter is used and the decomposition level is set to 9. No single wavelet transform has a statistically significant advantage over other wavelets in performance of the proposed hybrid method for PQM problems. If the harmonic components in the signal are perfectly localized, then the interpretation of the wavelet coefficients is rather difficult because of the Heisenberg uncertainty principle [21]. This principle implies that if the variance of a signal in the time domain $f(t)$ is σ_t , the variance of the signal in the frequency domain $f(f)$ is σ_f , and $||f|| = 1$, then the product $\sigma_t \sigma_f$ is at least 0.5. In the wavelet transform, there is a natural limit to the localization of the time and frequency. Therefore, energy levels of the detail coefficients are used instead of using raw coefficients after each decomposition level. The energy level of each of the detail coefficients is calculated using Eq. (4).

$$d_{1-9}Energy = \sum_{k=1}^{N/2} d_{1-9}^2 \tag{4}$$

In Eq. (4), N is total number of samples of the data window and d_{1-9} are the detail coefficients for each level. The input signal $x(t)$ is a 3-phase voltage signal and is supposed to be real-valued. In order to refrain from numerically high magnitudes, each energy level is normalized as:

$$d_{1-9 \text{ norm}} = \frac{f_s}{10^6} d_{1-9 \text{ Energy}}. \tag{5}$$

In Eq. (5), f_s is the sampling frequency. Useful features are extracted from the decomposed signals, which are used to recognize the type of PQDs. The DWT itself is not adequate to identify the type of PQDs since detail coefficients are highly affected by the power frequency. This is illustrated in Figure 2.

In Figure 2, the system frequency is chosen as 50 Hz, and the analyzed signal is a pure sine wave. It can be seen from Figure 2 that the energy levels of the d_8 and d_9 coefficients, which correspond to 50-100 Hz and 25-50 Hz, do not change. Provided that the power frequency does not change over time, the detail coefficient can be effectively used for identifying the PQDs. However, it is well known that power frequency can change over time by ± 1.5 Hz. This will yield variations of the detail coefficients. This phenomenon is illustrated in Figure 3. The analyzed signal is again a pure sine, but the power frequency is 49.8 Hz. It can be seen from Figure 3 that the energy levels of the d_8 and d_9 coefficients change over time, and in this case, these coefficients

cannot be used for PQ identification because they have a similar variation during a voltage sag/swell condition. The proposed algorithm uses a rectangular window with 512 samples in the DWT calculation. If the power frequency deviates from 50 Hz, the number of samples in the data window differs from 512 samples. For this reason, the d_8 and d_9 curves change over time and are hardly used.

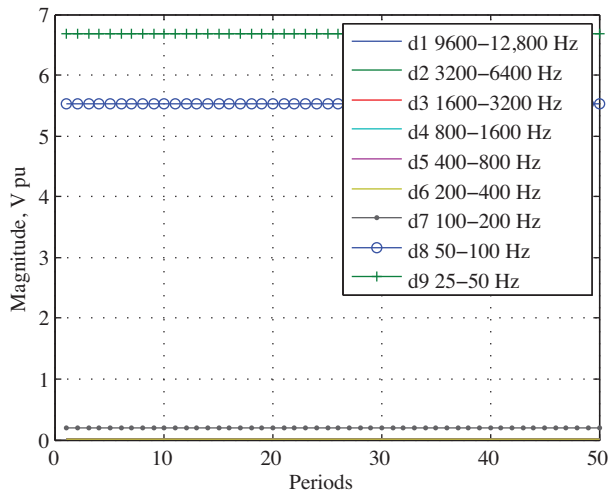


Figure 2. Detail coefficients of the analyzed signal for the system frequency of 50.0 Hz.

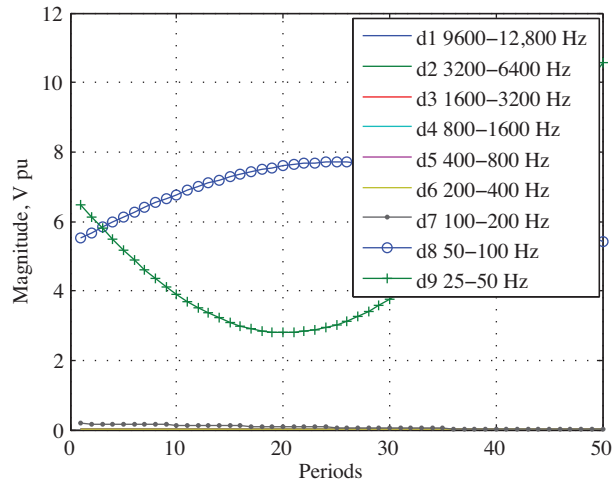


Figure 3. Detail coefficients of the analyzed signal for the system frequency of 49.8 Hz.

A previous study [17] in the literature uses the detail coefficients for feature extraction, assuming that the power frequency does not change from 50 Hz. However, power system frequency can deviate from 50 Hz by ± 0.5 Hz. This causes the sharp slopes in the detail coefficients of the analyzed signal. In this case, it is hard to define upper limits and lower limits for threshold values. In order to solve this problem, a new signal processing technique, PCA, is used. PCA has an offline training procedure, and so it cannot be affected if the system frequency changes. PCA is trained with d_8 and d_9 coefficients. If the same curves are applied to a successfully trained PCA, the decision-making unit will identify the pure sine wave with a slight change in power frequency as the normal operating condition. The following section gives a brief explanation of PCA.

3. Principal component analysis

PCA is a lower-dimensional projection method that can use multivariate data mining. The main idea behind PCA is to represent multidimensional data with fewer numbers of variables while retaining the main features of the data. The PCA method tries to project multidimensional data to a lower dimensional space while retaining the variability of the data as much as possible. PCA is also a useful statistical technique for face recognition and image compression. It is a common technique for finding patterns in data of high dimensions [25,26]. The main idea of PCA is to reduce dimensionality without losing too much information, in addition to finding a canonical representation of the data and preserving the variance of the data. The following examples, *step1* and *step2*, are useful for understanding the concept of the PCA algorithm.

step1: Projecting a point (data vector) into a lower dimensional space using PCA.

1. Let the data vector be x , and $x \in R$, $x = [x_1, x_2, \dots, x_n]$.
2. Select a basis. Let the basis vectors be $u = [u_1, u_2, \dots, u_n]$.

An orthonormal basis is considered with the following condition: $u_i \cdot u_i = 1$, and $u_i \cdot u_j = 0$ for $i \neq j$.

3. Select a center \bar{x} , which defines the offset of the space.
4. The best coordinates in the lower dimensional space are defined by dot products as:

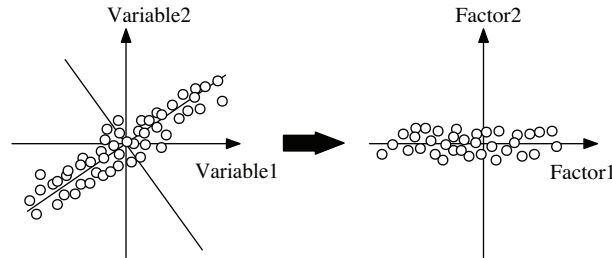


Figure 4. Rotating the coordinate frame in order to maximize the variance of the projections.

$$(z_1, z_2, \dots, z_k), \quad z_i = (x - \bar{x}) \cdot u_i. \quad (6)$$

It is required to find the direction of z_i , which maximizes the variance and minimizes the mean square error. As is seen in Figure 4, PCA is a linear transformation that transforms the data into a new coordinate system such that the direction with the greatest variance lies on the first coordinate, the second greatest variance on the second coordinate, and so on [27].

step2: The basic PCA algorithm is defined in the steps given below.

1. Reading the data matrix of x by $m \times n$ ($76,800 \times 6$). The first group of data (half of the matrix) is composed of voltage samples, and the other half of current samples.
2. Recentering procedure by subtracting the mean value from each row of data x .

$$x_c = x - \bar{x} \quad (7)$$

3. Computing the covariance matrix.

$$Cov = \frac{1}{m} \sum_{i=1}^m (x_{c(i)} - \bar{x})(x_{c(i)} - \bar{x})^T \quad (8)$$

4. Finding eigenvalues and eigenvectors of Cov from Eq. (8).
5. Selecting the k th eigenvectors with the highest eigenvalues (principal components). Note that the covariance matrix can be very large; therefore, finding eigenvectors may take too much computer time. In order to overcome this problem, the singular value decomposition (SVD) is used to calculate the k th eigenvectors. The following subsection gives a brief explanation of the SVD.

3.1. SVD calculation

The general SVD form is defined as:

$$x = WSV^T, \tag{9}$$

where x is the data matrix with 1 row per data point; W is the weight matrix with an $m \times m$ matrix of eigenvectors of xx^T – coordinate of x^i in eigenspace; S is the singular value matrix, diagonal matrix (in our setting, each entry is eigenvalue λ_i), i.e. n diagonal elements contain the square root of the eigenvalues of $x^T x$ or xx^T , and all of the other elements are 0; and V^T is the singular vector matrix (in our setting, each row is eigenvector v_j), i.e. rows of V contain the coefficients of the principal components.

The product of WS contains scores of the principal components, which is the amount each observation contributes to the principal components.

3.2. Residual generation

The first stage is data manipulation. The data are constructed in a dynamic way under normal working conditions from the samples of the system inputs $x(k)$ as:

$$x = [x_{k-l+1}^T \quad x_{k-l+2}^T \quad \dots \quad x_k^T]^T, \tag{10}$$

where l denotes the system order and x contains input data with a length of k . Since different variables in engineering systems usually use different units, the columns of x usually need to be scaled. Thus, they have zero mean and unity variance [28]. In the second stage, which is the offline stage, the covariance matrix is calculated using the autoscaled matrix as:

$$Cov = \frac{x^T x}{N - 1}, \tag{11}$$

where x shows the autoscaled data matrix and N is the total number of samples. To calculate the principal components, the eigenvectors and eigenvalues of the covariance matrix are computed and arranged in decreasing order of eigenvalues. The eigenvectors of the autoscaled covariance matrix are called principal components and they are used for residual generation purposes. In the last stage, the online residual generation stage, each new observation vector is autoscaled using the means and variances obtained in the offline stage and projected on to the principal component subspace. A residual vector at discrete time k is then calculated, using a few principal components, as:

$$e_k = \left\| x_m - \hat{x} \right\|^2 = \left\| (I - W_1 W_1^T) x_m \right\|^2, \tag{12}$$

where x_m shows the measurement vector and \hat{x} is called the prediction of the measurement vector. In a different way, the residual vector e at discrete time k is calculated using a few principal components related to the error matrix W_2 as:

$$e_k = \left\| W_2 W_2^T x_m \right\|^2. \tag{13}$$

The residual vector e_k is applied to the decision-making unit as an input. It has low magnitudes for no disturbance conditions and high magnitudes during any power system disturbance. The decision-making unit produces decisions about the type and degree of PQDs, such as the starting and ending of the disturbances and the magnitudes of the disturbances.

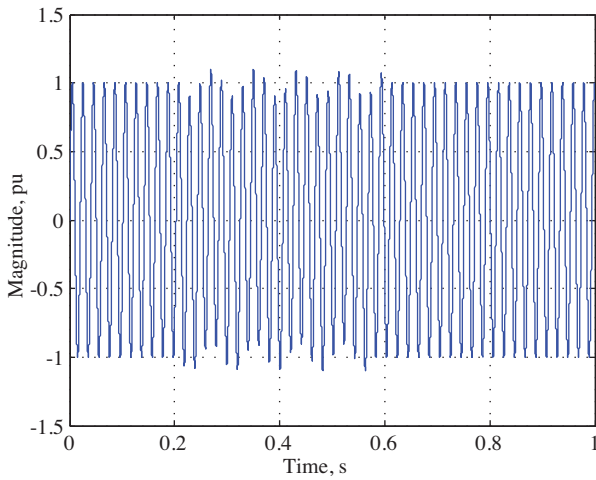


Figure 5. A normalized voltage signal with a flicker of 12 Hz, 0.1 pu.

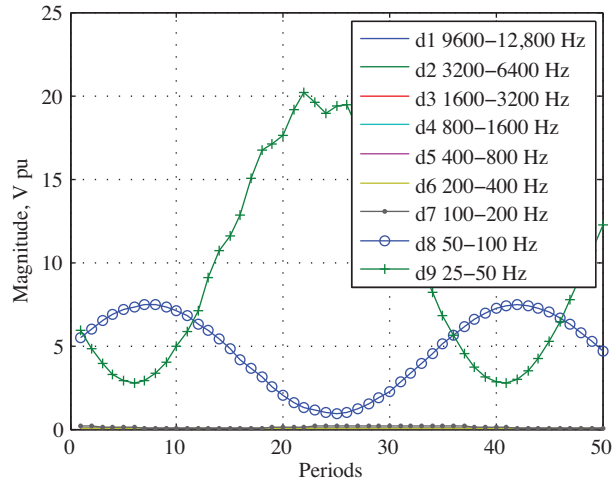


Figure 6. The detail coefficients of the analyzed signal ($f = 49.28$ Hz) with a flicker ($f_l = 12$ Hz, 0.1 pu).

The use of feature vectors based on the DWT and PCA is adequate to decide voltage sag/swell, momentary interruptions, harmonics, and electromagnetic interference, but it is not capable of identifying a voltage flicker condition. During a voltage flicker, it is observed that the signal has local maximums and minimums. Traditional classifiers identify this as voltage sag or swell on the analyzed signal. To correctly identify the condition, local maximums and minimums are calculated and used as feature vectors in the decision-making unit. Figure 5 shows the signal with a flicker of 12 Hz and 0.1 pu, and its calculated total envelope. The total envelope of the signal is the summation of the positive and negative peaks (local maximums and minimums). Here, the disturbance starts at the 12th period and ends at the 30th period. Figure 6 shows the detail coefficients of the analyzed signal (power frequency = 49.8 Hz) with a flicker frequency of 12 Hz and magnitude of 0.1 pu. The detail coefficients of Figure 6 are almost identical to those in Figure 3. The PCA output of this signal is nearly the same, as well. Therefore, the total envelope of the signal is included in the decision-making unit. Section 4 gives useful information about the decision-making unit and the whole calculation process.

4. Definition of the calculation procedure and the decision-making unit

The proposed hybrid algorithm for the detection of PQDs is first tested with artificially generated signals. The following subsections explain the whole calculation process.

4.1. Calculation process

1) In order to simulate real-time power signals, the power frequency and flicker frequency are randomly selected in simulations. The range for the power frequency is defined as ± 0.3 Hz and the flicker frequency is defined as between 5 and 25 Hz, which allows more realistic values to be obtained in the computer simulations.

2) The positive and negative peaks (local maximums and minimums) are calculated as:

$$\begin{aligned} xx &= x(1 + N * (k - 1) : N * k), \\ pos(k) &= \max(xx), \\ neg(k) &= \min(xx). \end{aligned} \quad (14)$$

In Eq. (14), xx is the per data frame, N is the number of samples in a period, pos and neg are the respective positive and negative peaks of the signal, and $k= 1$ to 25,600. The total envelope of the signal is obtained as:

$$Total = pos + neg. \tag{15}$$

The number of peaks of pos , neg , and $Total$ are then calculated. This procedure is required to identify a flicker condition.

3) The DWT is applied for each data window, and the detail coefficients are obtained for 9 levels. The energy levels of the detail coefficients are calculated and normalized as in Eqs. (4) and (5). The use of the DWT is summarized in Section 2.

4) PCA is used for analyzing the energy levels of the detail coefficients. A 3-phase pure sine signal (balanced and 50.0 Hz) is used for offline training of the PCA module. The manipulation steps can be summarized as follows:

- Read 3-phase pure sine signal.
- Read 3-phase real-time signal.
- Obtain a dynamic data set using a pure sinusoidal signal. In the offline procedure, the data matrix x 's mean and variances are first calculated. It is also autoscaled (i.e. zero mean, unity variance) using means and variances calculated before constructing the correlation matrix.
- Calculate the covariance matrix.
- Calculate the principle components and eigenvectors of the covariance matrix.
- Obtain a dynamic data set for a real-time signal. In the online fault monitoring stage, each new observation vector is autoscaled using the means and variances obtained in the offline stage and projected onto the principal component subspace.
- Calculate the residual (error) vector.

The use of PCA is summarized in Section 3. The correlation between the DWT and PCA is given in Table 1.

Table 1. Normalized energy levels of the detail coefficients and corresponding PCA outputs.

Normalized energy levels of the detail coefficients	PCA outputs
d1_norm (6400-12,800 Hz)	xr1
d2_norm (3200-6400 Hz)	xr2
d3_norm (1600-3200 Hz)	xr3
d4_norm (800-1600 Hz)	xr4
d5_norm (400-800 Hz)	xr5
d6_norm (200-400 Hz)	xr6
d7_norm (100-200 Hz)	xr7
d8_norm (50-100 Hz)	xr8
d9_norm (25-50 Hz)	xr9

4.2. Decision-making unit

The decision-making unit uses a set of crisp rules based on threshold values. The threshold values are applied to PCA outputs obtained from the DWT analysis. Since the DWT coefficients are scaled to relatively low magnitudes, the threshold value changes between 0 and 14 for PQM problems. These set values, 0→14, are determined empirically after numerous computer simulations and can easily be applied to real-time test data if the analyzed signal (voltage/current) is normalized to ± 1 . This unit produces 9 decisions: no disturbance, voltage sag, voltage swell, flicker, harmonics, transients, DC component, electromagnetic interference, and momentary interrupt. The rules are given as follows:

1) **IF** number of peaks of $Total > 1$ **and** $mean(pos) \neq 1$ **and** $mean(neg) \neq 1$ **and** $mean_value_of (Total)$ **THEN** ‘no disturbance’ **OTHERWISE** ‘disturbance detected’. If ‘no disturbance’ is detected, the algorithm runs the power frequency calculation algorithm for each period [29]. The details of this algorithm can be found in the Appendix. If the power frequency is calculated as 50 ± 0.1 Hz, the decision is again repeated as ‘no disturbance’. Otherwise, the frequency information is saved for postprocessing and the decision is changed as ‘frequency distortion’. The saved frequency information gives the user period by period frequency knowledge of the analyzed signal.

2) **IF** $\max(pos) < 0.999$ **and** $\max(neg) > -1$ **and** $\max(xr8) > 0.02$ **THEN** ‘voltage sag’. The value of voltage sag is calculated as:

$$V_{sag} = \frac{\max(pos) - \min(pos)}{\max(pos)}. \quad (16)$$

3) **IF** $\max(pos) > 1$ **and** $\max(neg) < -1$ **and** $\max(xr8) > 0.5$ **THEN** ‘voltage swell.’ The value of voltage swell is calculated as in Eq. (17).

$$V_{swell} = \frac{\max(pos) - \min(pos)}{\min(pos)} \quad (17)$$

4) **IF** Maximum number of positive peaks of $Total > 2$ **and** Maximum number of negative peaks of $Total > 2$ **THEN** ‘voltage flicker.’ The magnitude of the flicker is calculated as in Eq. (18).

$$Flicker_mag = 0.5 \frac{(\max(pos) - 1)}{(\min(neg) - 1)} \quad (18)$$

The flicker frequency is calculated using the FFT. In the frequency domain, a region of frequency between 0 and 46.66 Hz is searched to find the flicker frequency. However, the flicker frequency is randomly chosen as 5-25 Hz in this study. The maximum value of the frequency component in the scanned region is assigned as the flicker frequency.

5) **IF** $\max(xr7) > 0.1$ **and** $\max(xr6) > 0.015$ **THEN** ‘harmonics’. The FFT approach is again used for calculating voltage/current harmonics. Up to the 11th harmonic component is calculated in the FFT array. As soon as the harmonic components are calculated, the 3-phase unbalance factor and total harmonic distortions are calculated.

$$\%d = \frac{V_{\max} - V_{\min}}{V_{rated}} \quad (19)$$

In Eq. (19), d is a 3-phase unbalance factor in percent, V_{max} and V_{min} are the maximum and minimum values of the voltage signal, and V_{rated} is the rated value of the voltage signal. Eq. (20) gives the total harmonic

distortion for the voltage and current signals.

$$THD_v = \frac{\sqrt{\sum_{k=2}^{11} V_k^2}}{V_1} \text{ and } THD_i = \frac{\sqrt{\sum_{k=2}^{11} I_k^2}}{I_1} \tag{20}$$

In Eq. (20), V_1 and I_1 are the fundamental voltage and current harmonic components, respectively, and k is the order of the harmonics.

6) **IF** $\max(xr3) > 1.5E-3$ **and** $\max(xr8) > 0.01$ **and** $\max(xr9) > 0.01$ **THEN** ‘transients’.

7) **IF** number of positive (pos) peaks > 3 **and** number of negative (neg) peaks $= 0$ **and** $\max(xr8) > 0.1$ **THEN** ‘DC component’

OR

IF number of positive (pos) peaks $= 0$ **and** number of negative (neg) peaks > 3 **and** $\max(xr8) > 0.1$ **THEN** ‘DC component’. In the above **IF-THEN** statement, positive and negative DC components are detected. If a DC component is detected in the analyzed signal, the FFT is used for calculating its magnitude and variation with respect to time.

8) **IF** $\max(xr2) > 0.01$ **OR** $\max(xr1) > 0.01$ **THEN** ‘electromagnetic interference’.

9) **IF** $\max(\text{Total}) = 0$ **and** $\min(\text{Total}) \leq -0.9$ **and** $\max(xr8) > 9$ **and** $\max(xr9) > 14$ **THEN** ‘momentary interruption’. If any power system disturbance is detected, the beginning of the disturbance is calculated using pos and neg values. The variant from 1 and -1 of the pos and neg envelopes of the signal is scanned. Thus, the beginning of the disturbance is detected. The following condition is used for detecting the beginning of the disturbance:

IF number of pos > 1 **and** $\text{mean}(\text{pos}) \neq 1$ **and** $\text{mean}(\text{neg}) \neq -1$ **and** $\text{mean}(\text{top}) \neq 0$ **THEN** ‘find the variant from 1 and -1 of the pos and neg envelopes of the signal’.

5. Case studies

The case studies are divided into 2 groups. The first is based on a computer simulation using artificially generated power system signals. In order to simulate the real-time conditions, the fundamental system frequency and flicker frequency are selected randomly during the computer simulations. The duration of a disturbance is also selected randomly. Figure 7 shows the voltage sag example. The decision-making unit successfully identifies this condition as ‘voltage sag’. In the example given in Figure 7, the disturbance starts at 0.124 s and ends at 0.5 s. The calculated period of the beginning of the disturbance is 7 and the sag value is 0.1 pu. The power system frequency is randomly chosen to be 49.90 Hz. The following particular example belongs to a transient condition. The transient frequency is chosen as 3 kHz. Figure 8 shows the calculated values.

The decision-making unit identifies this condition successfully. The beginning of the disturbance is calculated to be the fourth period. A voltage swell condition is also detected as a disturbance and the value of the swell is given as 1.02 pu. In a real-time application, the data supplied by TÜBİTAK are used. This is an ongoing project devoted to taking the nationwide PQ figures of the Turkish electricity transmission system via field measurements carried out by application-specific mobile monitoring equipment. In this project, PQ measurements are being carried out according to IEC 61000-4-30, except the sampling rate, continuously during 7 days at the selected locations. In the transmission system, most of the bus bars have more than one incoming and outgoing feeder. Therefore, the number of measurement points can be taken as the number of feeders for currents and as the number of bus bars for voltages. The classification of these points as heavy industry, urban

+ industrial, and urban sites are given in Table 2 with respect to voltage level. It is noted that there are more than 95 incoming and outgoing feeders at the 33 measured transformer substations [4]. The real-time data are acquired in 3 s, which corresponds to 150 periods. Figure 9 shows the normalized real-time voltage signal with flicker. Figure 10 shows the total envelope of the signal under consideration. Figure 11 shows the DWT coefficients of the signal under investigation.

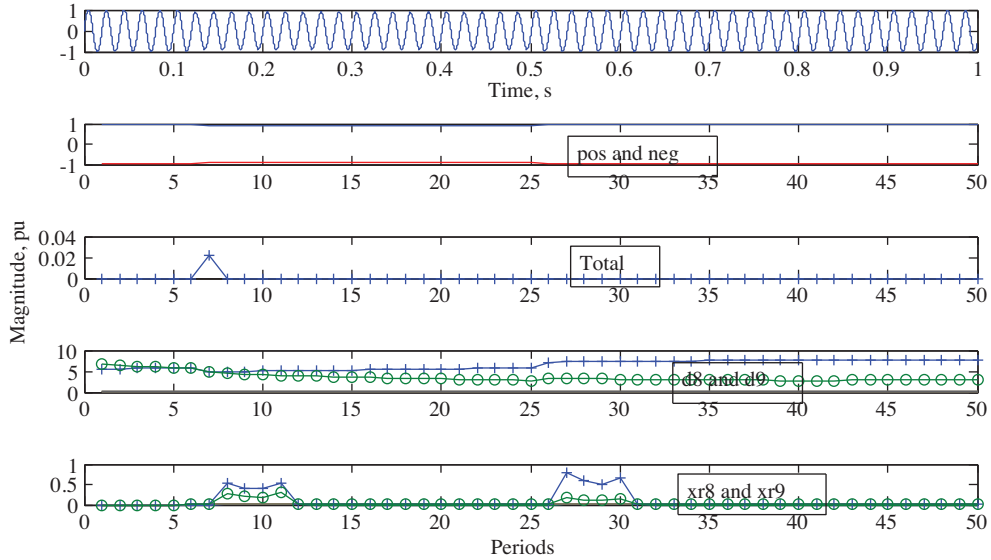


Figure 7. Voltage sag example.

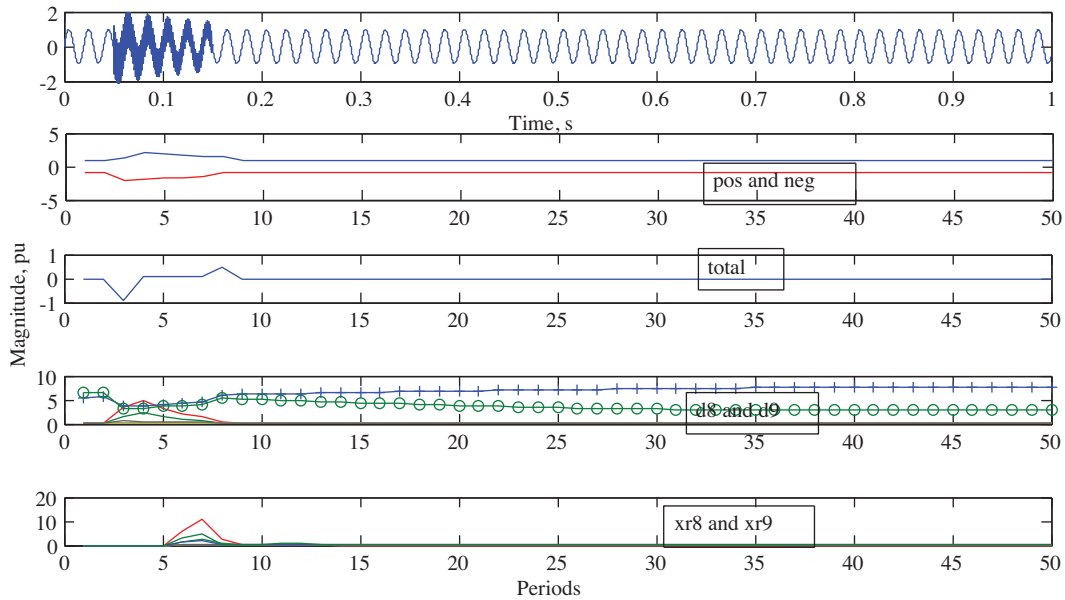


Figure 8. A transient condition example.

Since the calculated power system frequency is 50.2545 Hz, the related coefficients are not straightforward. In this particular example, the decision-making unit determines the beginning of the disturbance as the first period, the flicker frequency as 37 Hz, and the sag value as 0.29 pu. A number of real-time data obtained from

TÜBİTAK are investigated to evaluate the performance of the proposed hybrid algorithm. These studies have proven that the proposed algorithm is successfully able to identify PQ problems.

In Figure 11, there are only 2 visible lines, *d8* and *d9*, due to the scaling.

Table 2. Number of measurement points [4].

Number of measurement points								
Voltage level	Load type							
	Heavy industry		Industry urban		Urban only		Total	
	NB	NF	NB	NF	NB	NF	NB	NF
33 kV	8	16	17	28	14	16	39	60
154 kV	3	5	10	13	9	9	22	27
380 kV	1	1	4	7	0	0	5	8
Total	12	22	31	48	23	25	66	95

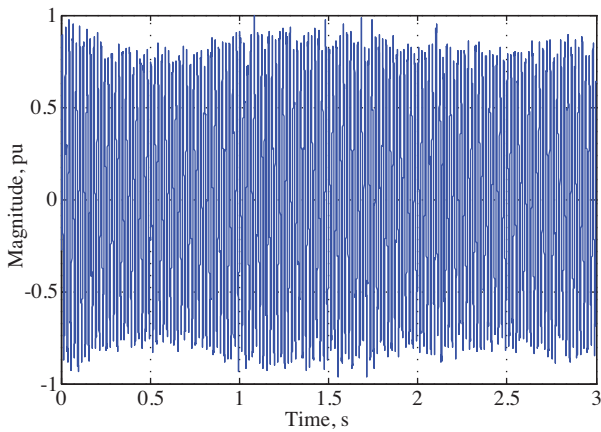


Figure 9. Real-time voltage signal with flicker.

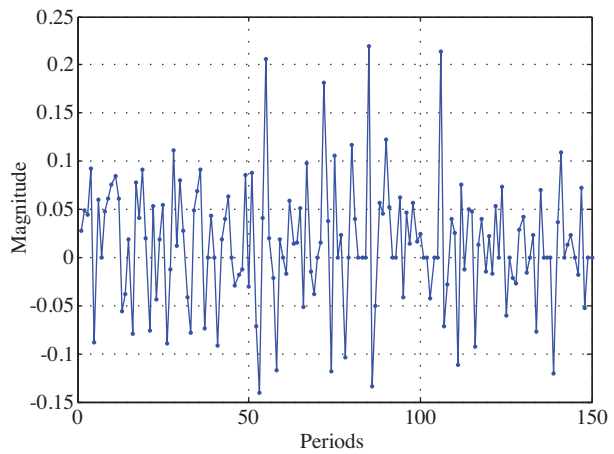


Figure 10. Total envelope of the voltage signal.

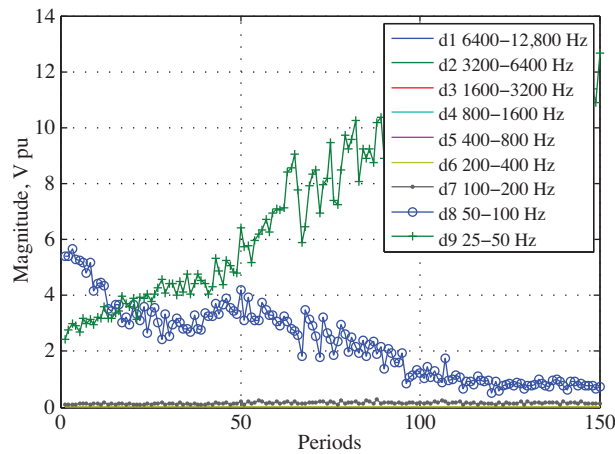


Figure 11. DWT coefficients of the voltage signal.

6. Conclusions

In this paper, a hybrid algorithm for the detection of PQ problems was proposed. The algorithm was capable of detecting and classifying many PQDs. The disturbance classification scheme was performed with the DWT, PCA, total envelope of the signal, and FFT approaches. A decision-making unit was used for classification based on crisp rules and it did not require other classification algorithms, such as a neural network or fuzzy classifiers. The proposed algorithm was applied to 2 sets of data, the first for generated data on a computer and the other for data obtained from TÜBİTAK. Practical applications showed that the proposed hybrid algorithm can be used in PQM software. The most important advantage of the suggested method is the reduction of the data size in the PCA unit. The DWT module was applied to 512 samples of data, while the FFT module was applied to 25,600 samples, to mitigate the effect of the spectral leakage problem. The PCA unit uses the first 5 singular values (square root of eigenvalues) of the 512 samples of the per data frame to produce feature vectors for the decision-making unit. Thus, it reduces memory space, shortens preprocessing requirements, and increases computational speed for the classification of PQDs. The analysis and results presented in this study clearly show the potential capability of the suggested hybrid algorithm in detecting and classifying the distorted PQ waveforms. In future work, the proposed algorithm will be turned into a web-based power monitoring system. The entire system will be developed on a Java technology platform.

Acknowledgment

The authors would like to thank TÜBİTAK for supplying real-time data.

References

- [1] T.D. Unruh, "Application techniques for power quality monitoring", IEEE/PES Transmission and Distribution Conference and Exposition, pp. 1-2, 2008.
- [2] Z. Hongliang, "GPRS based power quality monitoring system", Proceedings of the IEEE International Conference on Networking, Sensing and Control, pp. 496-501, 2005.
- [3] E. Özdemirci, Y. Akkaya, B. Boyrazoğlu, S. Buhan, A. Terciyanlı, Ö. Ünsar, E. Altıntaş, B. Haliloğlu, A. Açık, T. Atalık, Ö. Salor, T. Demirci, I. Çadırcı, M. Ermiş, "Mobile monitoring system to take PQ snapshots of Turkish electricity transmission system", Proceedings of the Instrumentation and Measurement Technology Conference, pp. 1-6, 2008.
- [4] T. Demirci, A. Kalaycıoğlu, Ö. Salor, S. Pakhuylu, T. İnan, D. Küçük, M. Güder, T. Can, Y. Akkaya, S. Bilgen, I. Çadırcı, M. Ermiş, "National power quality monitoring network and assessment center for the Turkish electricity transmission system: recent developments", IEEE 16th Signal Processing, Communication and Applications Conference, pp. 1-4, 2008.
- [5] P. Santarius, P. Krejci, Z. Chmelikova, J. Ciganek, "Long-term monitoring of power quality parameters in regional distribution networks in the Czech Republic", 9th International Conference on Harmonics and Quality of Power, pp. 1-5, 2008.
- [6] Y.H. Chen, M.J. Cheng, L.C. Hwang, J.H. Teng, "Embedded web server based power quality recorder", Proceedings of the IEEE Region 10 Conference, pp. 1-6, 2005.

- [7] Z. Lu, J.S. Smith, H. Wu, J. Fitch, "Empirical mode decomposition for power quality monitoring", IEEE/PES Transmission and Distribution Conference and Exhibition: Asia and Pacific, pp. 1-5, 2005.
- [8] M.A. Eldery, E.F. El-Saadany, M.M.A. Salama, A. Vannelli, "A novel power quality monitoring allocation algorithm", IEEE Transactions on Power Delivery, Vol. 21, pp. 768-777, 2006.
- [9] M.E. Salem, A. Mohamed, S.A. Samad, R. Mohamed, "Development of a DSP-based power quality monitoring instrument for real-time detection of power disturbances", International Conference on Power Electronics and Drives Systems, pp. 304-307, 2005.
- [10] D. Hong, J. Lee, J. Choi, "Power quality monitoring system using power line communication", Fifth International Conference on Information, Communications and Signal Processing, pp. 931-935, 2005.
- [11] W. Kang, X. Yan, H. Li, L. Zhang, "Design and realization of power quality monitoring system based on DSP and PCI technique", 12th International Power Electronics and Motion Control Conference, pp. 420-424, 2006.
- [12] V.A. Tukhas, S.A. Eintrop, "System of monitoring power quality parameters in real time", 9th International Conference on Electrical Power Quality and Utilization, pp. 1-3, 2007.
- [13] Y. Bi, J. Zhao, D. Zhang, "Research on power communication network and power quality monitoring using OPNET", Industrial Electronics and Applications, pp. 507-511, 2007.
- [14] H. Yang, Z. Bi, "The power quality monitoring system based on virtual instrument", World Congress on Software Engineering, pp. 243-245, 2009.
- [15] B.E. Kushare, A.A. Ghatol, S. Kala, "Development of web based power quality monitoring system for handling user custom power quality query and auto power quality monitoring report notification via email", IET-UK Information and Communication Technology in Electrical Sciences, pp. 1-7, 2007.
- [16] K. Yingkayun, S. Premrudeepreechacharn, K. Oranpiroj, "A power quality monitoring system for real-time fault detection", IEEE International Symposium on Industrial Electronics, pp. 1846-1851, 2009.
- [17] Z. Moravej, A.A. Abdoos, M. Pazoki, "Detection and classification of power quality disturbances using wavelet transform and support vector machines", Electric Power Component and Systems, Vol. 38, pp. 182-196, 2010.
- [18] H. He, H. Zhang, "A new power quality monitoring system based on ARM and SOPC", ISECS International Colloquium on Computing, Communication, Control, and Management, pp. 24-27, 2008.
- [19] A.A. Girgis, "Measurement of voltage flicker magnitude and frequency using a Kalman filtering based approach", Canadian Conference on Electrical and Computer Engineering, pp. 659-662, 1999.
- [20] C.J. Wu, Y.J. Chen, "A novel algorithm for precise voltage flicker calculation by using instantaneous voltage vector", IEEE Transaction on Power Delivery, Vol. 21, pp. 1541-1548, 2006.
- [21] G. Strang, T. Nguyen, Wavelets and Filter Banks, Wellesley, Massachusetts, Wellesley-Cambridge Press, 1996.
- [22] O. Ozgonenel, D.W.P. Thomas, C. Christopoulos, "Modelling and identifying of transformer faults", IEEE Russia Power Tech, pp. 1-7, 2005.
- [23] I. Daubechies, Ten Lectures on Wavelets, Philadelphia, Society for Industrial and Applied Mathematics, 1992.

- [24] O. Ozgonenel, E. Kilic, D.W.P. Thomas, A.E. Ozdemir, "Identification of transformer internal faults by using an RBF network based on dynamical principle component analysis", The First International Conference on Power Engineering, Energy and Electrical Drives, pp. 719-724, 2007.
- [25] G.T. Heydt, A.W. Galli, "Transient power quality problems analyzed using wavelets", IEEE Transactions on Power Delivery, Vol. 12, pp. 908-991, 1997.
- [26] H. Vedam, V. Venkatasubramanian, "PCA-SDG based process monitoring and fault diagnosis", Control Engineering Practice, Vol. 7, pp. 903-917, 1999.
- [27] H. Zang, A.K. Tangirala, S.L. Shah, "Dynamic process monitoring using multiscale PCA", IEEE Canadian Conference on Electrical and Computer Engineering, Vol. 3, pp. 1579-1584, 1999.
- [28] L.I. Smith, A Tutorial on Principal Components Analysis, Dunedin, New Zealand, Department of Computer Science of University of Otago, 2002. Available at http://www.cs.otago.ac.nz/cosc453/student_tutorials/principal_components.pdf (accessed 3 May 2010).
- [29] C. Kocaman, O. Ozgonenel, M. Ozdemir, U.K. Terzi, "Calculation of fundamental power frequency for digital relaying algorithms", Developments in Power System Protection Conference, pp. 1-5, 2010.
- [30] E.Y. Hamid, Z.I. Kawasaki, "Wavelet based data compression of power system disturbances using the minimum description length criterion", IEEE Transactions on Power Delivery, Vol. 17, pp. 460-466, 2002.